Iris Recognition: Analyzing the Distribution of the Iriscodes Concordant Bits

Gil Santos and Hugo Proença
Department of Computer Science
Instituto de Telecomunicações - Networks and Multimedia Group
University of Beira Interior, Covilhã, Portugal
Email: gmelfe@ubi.pt, hugomcp@di.ubi.pt

***Abstract*—The growth in practical applications for iris biometrics has been accompanied by relevant developments in the underlying algorithms and techniques. Efforts are being made to minimize the tradeoff between the recognition error rates and data quality, acquired in the visible wavelength, in less controlled environments, over simplified acquisition protocols and varying lighting conditions. This paper presents an approach that can be regarded as an extension to the widely known Daugman's method. Its basis is the analysis of the distribution of the concordant bits when matching iriscodes on both the spatial and frequency domains. Our experiments show that this method is able to improve the recognition performance over images captured in less constrained acquisition setups and protocols. Such conclusion was drawn upon trials conducted for multiple datasets.**

I. Introduction

The use of the iris as main biometric trait is emerging as one of the most recommended, due not only to the possibility of contactless data acquisition and to its circular and planar shape that makes easy the detection, segmentation and compensation for off-angle capturing, but also for its predominately randotypic appearance. Although these factors contribute to the high effectiveness of the deployed iris recognition systems, their typical scenarios are quite constrained: subjects stop-and-stare relatively close to the acquisition device, while their eyes are illuminated by a near-infrared light source, enabling the acquisition of good quality data. Remarkably, several researchers are trying to minimize the constraints associated with this process, in a way often referred as *non-cooperative iris recognition*.

Traditional iris recognition methods are based on the statistical Pattern Recognition paradigm and regard the biometric signatures as points of hyper-dimensional spaces. Here, a match occurs when the distance between two signatures is lower than a threshold. However, dealing with degraded data might lead to huge deformations of the feature space and significant increases of the error rates. In this paper we propose a method that accounts for the spatial and frequency analysis of the bits that are in agreement when comparing two biometric signatures (iriscodes). The goal is to increase the robustness to degraded data, captured in unconstrained acquisition setups. The Daugman's approach, widely known for it's low error rates and commercially deployed in iris recognition systems worldwide, has proven to perform well in different types of images and, therefore, will be the basis of our work and our comparison term.

The remaining of this paper has the following structure: section II overviews the iris recognition process, namely the less constrained acquisition setup and the Daugmans's approach; section III describes the proposed method; section IV describes the used datasets and discusses the obtained results; finally, section V states the conclusions.

II. Iris Recognition

The iris recognition process starts with the segmentation of the iris ring. Further, data is transformed into a double dimensionless polar coordinate system, through the *Daugman's Rubber Sheet* process. Regarding the feature extraction stage, existing approaches can be roughly divided into three variants: phase-based [1], zero-crossing [2] and texture-analysis methods [3]. Dauman [1] used multi-scale quadrature wavelets to extract texture phase-based information and obtain an iris signature with 2048 binary components. Boles and Boashash [2] computed the zero-crossing representation of a 1D wavelet at different resolutions of concentric circles. Wildes [3] proposed the characterization of the iris texture through a Laplacian pyramid with four different levels. Finally, in the feature comparison stage, a numeric dissimilarity value is produced, which determines the subjects identity. Here, it is usual to apply different distance metrics (Hamming [1], Euclidian [4] or weighted Euclidian [5]), or methods based on signal correlation [3].

The accuracy of the deployed iris recognition systems is remarkable, as reported by the study conduced by Daugman [6] and three other independent evaluations [7]–[9]. Nevertheless, recent publications emphasize the significance of some iriscode bits [10], aiming at improving by either masking less consistent bits [11] or condensing high discriminatory information regions [12]. However, we stress that the claimed effectiveness is conditioned to the acquisition of good quality images, captured in stop-and-stare interfaces at reduced imaging distances. In less constrained conditions, where a trade-off between data acquisition constrains and recognition accuracy is inevitable, the challenge is to maximally increase flexibility in three axes: subjects position and movement, imaging distances and lighting conditions. The main problem

is the appearance of other noise factors [13] (Subsection IV-A), that represent a substantial issue. As before stated, this area receives growing interests from the research community and constituted the scope of several publications [14]–[16].

A. Daugman's Approach

The Daugman's approach [17] to perform iris recognition is the most widely acknowledged, with great acceptance over the scientific community. Apart from being the unique implemented in commercially deployed systems, it usually acts as comparison term for alternative proposals. His method starts by the detection and segmentation of the iris. Later, the normalization of the segmented region is performed and features are extracted through the convolution of the normalized data with a bank of 2D Gabor Wavelets (1), followed by a quantization stage that produces a binary *iriscode*. This code is used in the matching stage, that applies the *Hamming* distance (3) as comparison measure.

$$h_{\{Re,Im\}} = sgn_{\{Re,Im\}} \int_{\rho}\int_{\phi} I(\rho,\phi) e^{iw(\theta_0-\phi)}. \\ .e^{-(r_0-\rho)^2/\alpha^2} e^{-(\theta_0-\phi)^2/\beta^2} \rho d\rho d\phi \tag{1}$$

$$c = (codeA \otimes codeB) \cap maskA \cap maskB \tag{2}$$

$$HD = \frac{\|c\|}{\|maskA \cap maskB\|} \tag{3}$$

where $\otimes$ is the logical XOR operation and $\cap$ the logical AND.

III. Proposed Methdod

The similarity measure used by Daugman at the matching stage simply gives the ratio of concordant iriscode bits over the whole iris and does not take into account their spatial and frequency distributions. In this paper, such analysis is performed, hoping that the location of the concordant bits and how they spread in the iriscode can provide useful information in the discrimination between match and non-match comparisons.

(a) Iriscodes match with regular distributed concordant bits

(b) Iriscodes match with an high concordance region (delimited by the light gray rectangle)

Fig. 1. Illustration of two iriscode matching results. Black pixels express concordant bits in the corresponding biometric signatures.

Figure 1 illustrates two comparisons between iriscodes, from now on called "*comparison maps*" (2), where black pixels denote concordant bits of the corresponding biometric signatures. Although their Hamming Distance is the same (50% of concordant bits) we claim that - intuitively - the *comparison map* from Figure 1(b) has a much higher probability of being an intra-class comparison. This is due to the (delimited) region that gives an area where both iriscodes have high concordance.

A. Spatial Domain Analysis

To ascertain the level of concordance in regions of different sizes, we performed a set of convolutions with Haar-based wavelets of different sizes. Let c be a *comparison map* of $M \times N$ dimensions. Let h be a Haar-based mother wavelet with size $s \times s$. The similarity r in local regions of c is given by:

$$r_s = h_s * c \qquad , s = \{2k\},\ k = 2,3,...,16 \tag{4}$$

where $*$ denotes the bi-dimensional convolution and r_s has the same dimensions of c.

Let $\omega_s = \max\{r_s(i,j)\},\ i = 1,2,...,N;\ j = 1,2,...,M$.

Let H be the 25-bin histogram of $r_{\frac{\psi}{2}}$ where ψ is the maximum size of the Haar-wavelet, such that $H = \{h_1, h_2, ..., h_{25}\}$. All the ω_i and h_i values where used as fetures for the further stages (sub-section IV-B) and give the proportion of concordant bits across regions of different sizes of the comparison map.

B. Frequency Domain Analysis

Together with the above described analysis we also analyzed the frequencies spread of the concordant bits. The rationale is that matching between inter-class iriscodes should give a distribution close to white-noise of concordant bits. Oppositely, an intra-class comparison should present a higher amount of low frequency components, according to the same key insight given in the previous section.

At this stage, two modifications to the Daugman's approach were performed: remotion of the signal-wise binary conversion step; and replacement of the XOR operation by the difference between coefficients. When applying a Fourier transform to both the binary and the differential *comparison maps*, we found that the later produces more discriminating results, which is easily justified by its higher amount of information.

Let c be a *comparison map* of $M \times N$ dimensions. The 2D Fourier transform F is given by:

$$F(u,v) = \frac{1}{N} \sum_{x=0}^{M} \sum_{y=0}^{N} c(x,y) e^{-j2\pi(ux/M + vy/N)} \tag{5}$$

where j is the square root of -1 and e denotes the natural exponent.

Results were decomposed into sixteen sub-regions, regularly distributed in small windows, and a set of attributes was ascertained: minimum and maximum values, average, standard deviation and local entropy. Since the central shape of F (where the lower frequencies lie) might contain important information which could not be properly processed by this windowing, another method was used to extract specific features from this area.

Let A be a $P \times N$ window, centered in the $P \times M$ matrix that contains the noticeable central shape such that $P = 2M/8$. Ten features F_i are then extracted as explained in the initial

part of section (6b), representing the distribution of evenly spaced 10-bins histogram:

$$T_i = \min(A) + i\frac{\Delta A}{10} \tag{6a}$$

$$F_i = \sum_{m=1}^{P}\sum_{n=1}^{N} \operatorname{sgn}\left(A_{(m,n)} - T_i\right) \tag{6b}$$

with $\Delta A = \max(A) - \min(A)$ and $i = 1, 2, ..., 10$.

IV. Experiments

Thus, the required parameters of the Gabor wavelets (1) were tuned for best performance, being chosen those with maximal decidability index (7); *i.e.* maximizing the distance between the distributions obtained for the two classical types of biometric comparisons: between signatures extracted from the same (*intra-class*) and different eyes (*inter-class*).

$$d' = \frac{|\mu_{inter} - \mu_{intra}|}{\sqrt{\frac{\sigma^2_{inter} + \sigma^2_{intra}}{2}}} \tag{7}$$

where μ_{inter} and μ_{intra} denote the means of the inter- and intra-class comparisons and σ_{inter} and σ_{intra} the respective standard deviations.

Regarding iris segmentation, all images were manually segmented, avoiding that segmentation errors corrupt the obtained results. A central and contiguous region was extracted from the normalized image, free of eyelid and eyelash occlusions, and used for the extraction of the iriscode. This option was taken to empower the spatial and frequency domain analysis.

A. Datasets

Two different datasets were used in our experiments: UBIRIS [18] and UBIRIS.v2 [19]. These are noisy datasets [13] with the following factors that degrade the quality of the data:

- **Out-of-Focus** - caused by subject movement allied to imaging systems limitations (namely in the depth-of-field, poor lightning/exposure ratio);
- **Off-Angle** - subject head and eye rotation or lack of alignment;
- **Rotation** - tilt of the head, despite of the subject being or not facing the camera;
- **Motion blur** - blurred iris images caused by eyelid movement;
- **Obstructions** - various types of blocking objects can be found, being the most commons: eyelids, eyelashes, glasses and contact lenses;
- **Reflections** - generally strong reflections caused by light sources or weak ones introduced by surroundings;
- **Partial Iris** - images appear where iris is not completely visible;
- **Out-of-iris** - images where iris is not present at all, either because fully occlusions or the eye not being present in the frame.

The higher range of acquisition distances enables the capturing of data at different scales and should make the results more visible.

Four dataset configurations were employed:

- UBIRIS.v2 – the first one is made of 500 images from UBIRIS.v2 without any kind of particular selection;
- UBIRIS.v2 Frontal – a second arrangement consists of 175 images, also from UBIRIS.v2, captured with the subject looking at camera's direction;
- UBIRIS.v2 Frontal Close – the third setup is composed by 100 images from the same database, with the subject also looking at the camera, but at relatively closer distances (4 to 6 meters);
- UBIRIS – the last setup include 500 images from UBIRIS.

The number of comparisons c_n is given from the number of irises n in the database through (8), from which about 4.5% are intra-class comparisons. In every case, we selected a group of images that we believe to represent each dataset.

$$c_n = \sum_{i=1}^{n-1} i \tag{8}$$

B. Feature Selection and Classification

Upon trials using different feature selection and dimensionality reduction techniques, carried out on frontally captured irises, we decided to apply Logistic Regression (LR) to the best 125 features, sorted using Peng *et al*. method [20] - *minimum-Redundancy, Maximum Relevance*, and then mapped to 15 dimensions through *Local Fisher Discriminant Analysis* [21]. By conducting our earliest tests in an UBIRIS.v2 sub-set of frontal images, we avoided problems associated with others noise factors (as gaze look), which might require specific corrections.

C. Results and Discussion

When applied to the different datasets, the comparison of our method and of the Daugman's gave the results contained in tables I and II.

TABLE I
LOGISTIC REGRESSION RESULTS FOR DIFFERENT DATASET CONFIGURATIONS. "HD" REPRESENTS DAGUMAN'S APPROACH PERFORMANCE, AND "125 FEAT" REFERS TO OUR APPROACH. AUC STANDS FOR AREA UNDER ROC CURVE AND CA FOR CLASSIFICATION ACCURACY

	HD		125 Feat	
	AUC	CA	AUC	CA
UBIRIS.v2	0.7315	0.9574	0.7598	0.9589
UBIRIS.v2 Frontal	0.8499	0.9582	0.8562	0.9590
UBIRIS.v2 Frontal Close	0.8740	0.9632	0.8897	0.9643
UBIRIS	0.9865	0.9868	0.9932	0.9897

Starting by frontal UBIRIS.v2 images, the subset our method was initially projected on, and attending to *Area Under ROC Curve* (AUC) assessment, we can observe an apparently residual increment of 1%. However, the AUC differs from Daugman's approach from 1.57% on close-captured images

to 2.83% on images without restrictions of any kind, which is a more significative improvement. For the first version of UBIRIS, where Daugman's approach has a good performance considering acquisition conditions, our method once again presents enhancements of almost 1% (Figure 2).

For the *Classification Accuracy* (CA), more permeable to class unbalancing, the most notable boost occurs for UBIRIS, as for the second version of this database advancements are proportional to the ones of AUC.

TABLE II
CONFUSION MATRICES REPRESENTING PROPORTIONS OF TRUE FOR DIFFERENT DATASET CONFIGURATIONS. "HD" REPRESENTS DAUGMAN'S APPROACH PERFORMANCE, AND "125 FEAT" REFERS TO OUR APPROACH.

		Predicted			
		HD		125 Feat	
		0	1	0	1
UBIRIS.v2	Real 0	1.000	0.000	1.000	0.000
	Real 1	0.991	0.009	0.950	0.050
UBIRIS.v2 Frontal	Real 0	0.997	0.003	0.997	0.003
	Real 1	0.858	0.142	0.841	0.159
UBIRIS.v2 Frontal Close	Real 0	0.997	0.003	0.996	0.004
	Real 1	0.797	0.203	0.744	0.256
UBIRIS	Real 0	0.998	0.002	0.998	0.002
	Real 1	0.262	0.738	0.194	0.806

Table II allows us to interpret the results in a more perspicuous way. Having in mind the priority given to lower the *False Accept Rate* (FAR) as much as possible, is at the *False Reject Rate* (FRR) that the improvements due to our method can be better observed. Without jeopardizing the FAR, FRR has a drop of about 1.7% for the subset where our method was schemed, when compared to the information provided by HD alone. Analyzing the other two UBIRIS.v2 datasets, this drop became more suggestive reaching 4.1% to 5.3%, and 6.8% on UBIRIS.

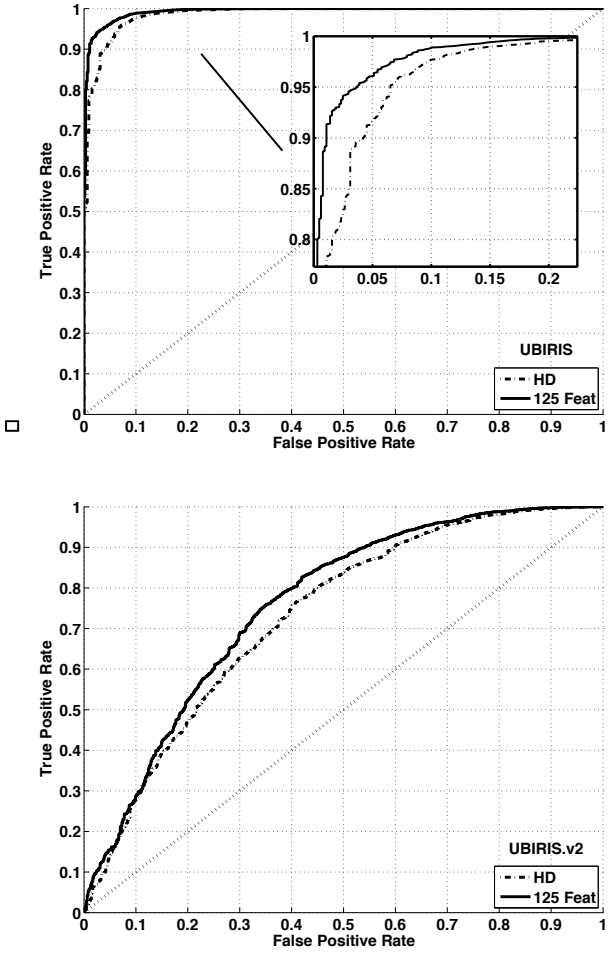

Fig. 2. ROC curves for UBIRIS and UBIRIS.v2 respectively. Inside curves represent Daugman's method (HD) result and outer ones refer to the proposed method (125 Feat).

V. CONCLUSIONS

Unconstrained image acquisition setups and protocols lead to the appearance of degraded data that significantly increases the challenges in performing accurate iris biometric recognition. In this paper we assessed the spatial and frequency distributions of the agreement bits resultant of the comparison between iriscodes having as main purpose the increase of the robustness to data acquired in less controlled conditions. Based in well-known feature extraction and data mining techniques, our method is to be used together with the traditional Daugman's approach and consistently contributed for an improvement in all experimented datasets.

ACKNOWLEDGMENT

We acknowledge the financial support given by "FCT-Fundação para a Ciência e Tecnologia" and "FEDER" in the scope of the PTDC/EIA-EIA/103945/2008 research project "NECOVID: Negative Covert Biometric Identification".

REFERENCES

[1] J. G. Daugman, "Phenotypic versus genotypic approaches to face recognition," in *Face Recognition: From Theory to Applications*. Heidelberg: Springer-Verlag, 1998, pp. 108–123.

[2] W. Boles and B. Boashash, "A human identification technique using images of the iris and wavelet transform," *Signal Processing, IEEE Transactions on*, vol. 46, no. 4, pp. 1185–1188, April 1998.

[3] R. P. Wildes, "Iris recognition: an emerging biometric technology," *Proceedings of the IEEE*, vol. 85, no. 9, pp. 1348–1363, September 1997.

[4] Y. Huang, S. Luo, and E. Chen, "An efficient iris recognition system," in *Proceedings of the First International Conference on Machine Learning and Cybernetics*, China, November 2002, pp. 450–454.

[5] L. Ma, T. Tan, Y. Wang, and D. Zhang, "Efficient iris recognition by characterizing key local variations," *Image Processing, IEEE Transactions on*, vol. 13, no. 6, pp. 739–750, June 2004.

[6] J. G. Daugman, "New methods in iris recognition," *Systems, Man, and Cybernetics, Part B: Cybernetics, IEEE Transactions on*, vol. 37, no. 5, pp. 1167–1175, October 2007.

[7] J. L. Cambier, "Iridian large database performance," Iridian Technologies, Tech. Rep., 2007, http://iridiantech.com.

[8] "Independent test of iris recognition technology," International Biometric Group, Tech. Rep., 2005, http://www.biometricgroup.com.

[9] T. Mansfiel, G. Kelly, D. Chandler, and J.Kane, "Biometric product testing and final report, issue 1.0," 2001.

[10] K. P. Hollingsworth, K. W. Bowyer, and P. J. Flynn, "The best bits in an iris code," *IEEE Transactions on Pattern Analysis and Machine Intelligence*, vol. 31, pp. 964–973, 2009.

[11] ——, "Using fragile bit coincidence to improve iris recognition," in *BTAS'09: Proceedings of the 3rd IEEE international conference on Biometrics: Theory, applications and systems*. Piscataway, NJ, USA: IEEE Press, 2009, pp. 165–170.

[12] J. E. Gentile, N. Ratha, and J. Connell, "Slic: short-length iris codes," in *BTAS'09: Proceedings of the 3rd IEEE international conference on Biometrics: Theory, applications and systems*. Piscataway, NJ, USA: IEEE Press, 2009, pp. 171–175.

[13] H. Proença and L. A. Alexandre, "The NICE.I: Noisy iris challenge evaluation - part i," in *Biometrics: Theory, Applications, and Systems, 2007. BTAS 2007. First IEEE International Conference on*, September 2007, pp. 1–4.

[14] J. R. Matley, D. Ackerman, J. Bergen, and M. Tinker, "Iris recognition in less constrained environments," *Springer Advances in Biometrics: Sensors, Algorithms and Systems*, pp. 107–131, October 2007.

[15] C. Fancourt, L. Bogoni, K. Hanna, Y. Guo, R. Wildes, N. Takahashi, and U. Jain, "Iris recognition at a distance," in *Proceedings of the 2005 IAPR Conference on Audio and Video Based Biometric Person Authentication*, U.S.A., July 2005, pp. 1–13.

[16] R. Narayanswamy, G. Johnson, P. Silveira, and H. Wach, "Extending the imaging volume for biometric iris recognition," *Applied Optics, vol. 44, no. 5*, pp. 701–712, February 2005.

[17] J. G. Daugman, "How iris recognition works," *Circuits and Systems for Video Technology, IEEE Transactions on*, vol. 14, no. 1, pp. 21–30, January 2004.

[18] H. Proença and L. A. Alexandre, "UBIRIS: A noisy iris image database," in *ICIAP*, September 2005, pp. 970–977.

[19] H. Proença, S. Filipe, R. Santos, J. Oliveira, and L. A. Alexandre, "The UBIRIS.v2: A database of visible wavelength images captured on-the-move and at-a-distance," *IEEE Transactions on Pattern Analysis and Machine Intelligence*, vol. 99, no. 1, 5555.

[20] H. Peng, F. Long, and C. Ding, "Feature selection based on mutual information: Criteria of max-dependency, max-relevance, and min-redundancy," *IEEE Transactions on Pattern Analysis and Machine Intelligence*, vol. 27, no. 8, pp. 1226–1238, August 2005.

[21] M. Sugiyama, "Local fisher discriminant analysis for supervised dimensionality reduction," in *ICML '06: Proceedings of the 23rd international conference on Machine learning*. New York, NY, USA: ACM Press, 2006, pp. 905–912.